

**SUPERPARAMAGNETIC IRON OXIDE NANOPARTICLES DEVELOPMENT,  
CHARACTERIZATION, CUPPER-64 LABELING AND CELLULAR  
TRACKING**

A Thesis  
Presented to  
The Academic Faculty

by

Nazanin Hoshyar Masoodzadehgan

In Partial Fulfillment  
of the Requirements for the Degree  
Master of Science in Medical Physics

Georgia Institute of Technology

May 2012

**SUPERPARAMAGNETIC IRON OXIDE NANOPARTICLES DEVELOPMENT,  
CHARACTERIZATION, CUPPER-64 LABELING AND CELLULAR  
TRACKING**

Approved by:

Dr. Gang Bao  
Coulter Department of Biomedical  
Engineering  
*Georgia Institute of Technology*

Dr. Tim Fox  
Department of Radiation Oncology  
*Emory University School of Medicine*

Dr. Farzad Rahnema  
Woodruff School of Mechanical Engineering  
*Georgia Institute of Technology*

Date Approved: Jan 11, 2012

## ACKNOWLEDGEMENTS

I am extremely grateful to Dr. Gang Bao for all his guidance, help and support. His patience and guidance as an advisor and mentor have been invaluable. I would like to thank the members of my thesis committee, Dr. Tim Fox and Dr. Farzad Rahnema, for their time and instruction. The funding for this project was provided through the National Institute of Health.

To the past and present members of Bao Lab, thank you for the foundation you have built and for your help with this research. In particular, I would like to thank Dr. Sheng Tong and Dr. Sijian Hue for being available to answer my many coating questions. This work would have been much more difficult without Dr. Johanness Leisen MRI help. I also would like to thank Annie for all her help with cellular studies and lab management.

Finally, I would like to thank my family for all their support and encouragement through the past few years. I would especially like to thank my husband Ata for his love and support.

## TABLE OF CONTENTS

ACKNOWLEDGEMENTS .....	iii
LIST OF FIGURES .....	v
NOMENCLATURE .....	vii
SUMMARY .....	xiv
CHAPTER 1: SYNTHESIS AND CHARACTERIZATION OF SPIO.....	1
1.1 Developing SPIO as an MR contrast agent.....	3
1.2 Particle Characterization.....	5
1.3 Particle Size .....	5
1.4 Circulation Half-life.....	7
CHAPTER 2: STEM CELL TRACKING.....	9
2.1 INTRODUCTION .....	9
2.2 SPIO DELIVERY.....	10
2.3 Measurement of Cell Iron Content.....	11
2.4 CYTOTOXICITY ASSAY .....	12
2.5 CONFOCAL MICROSCOPY .....	15
2.6 MRI of hMSCs.....	18
CHAPTER 3: DUAL MODALITY PET/MR CONTRAST AGENT.....	22
3.1 Dual Modality Nanoparticles for PET MR Imaging.....	23
3.2 Synthesis of DTPA SPIO.....	24
3.3 Radiolabeling of DTPA SPIO with <sup>64</sup> Cu .....	26
3.4 Serum Stability of <sup>64</sup> Cu-labeled SPIO.....	29
CHAPTER 4: DISCUSSION, CONCLUSION AND FUTURE WORK .....	32
4.1 Discussion and Conclusion.....	32
4.2 Future Work .....	33
REFERENCES .....	34

## LIST OF FIGURES

Figure 1.1. Schematic diagram of SPIO structure. The core is made of iron oxide with a combined coating of Oleic acid and oleylamine. The final coating is made of PEG. ....	2
Figure 1.2. Iron Oxide Cores synthesized using thermodecomposition of iron complex in organic solvents .....	3
Figure 1.3. TEM images of the coated SPIO using the dual-exchange solvent method. SPIOs were negatively stained with phosphotungstic acid to show a white layer surrounding the iron oxide cores indicating the DSPE-mPEG2000 coating layer. ....	4
Figure 1.4. Size distribution of iron core and coated SPIO using a DynaPro NanoStar Dynamic Light Scattering Instrument.....	6
Figure 1.5. Blood clearance of 17nm SPIOs after intravenous injection. Blood samples were collected by tail nicking at 5, 30, 60, 120, 180 and 240 minutes post injection of SPIO. Amount of iron in the blood was quantified with a Ferrozine Assay. Data is shown as percent injected dose. ....	8
Figure 2.1. Cell Viability Assay of hMSCs after incubating with SPIO (labeled with media containing Fe: 0 $\mu\text{g}/\text{ml}$ , 50 $\mu\text{g}/\text{ml}$ , 100 $\mu\text{g}/\text{ml}$ , and 200 $\mu\text{g}/\text{ml}$ ) for 24 hours .....	13
Figure 2.2. Cell Viability Assay of hMSCs after incubating with SPIO (labeled with media containing Fe: 0 $\mu\text{g}/\text{ml}$ , 50 $\mu\text{g}/\text{ml}$ , 100 $\mu\text{g}/\text{ml}$ , and 200 $\mu\text{g}/\text{ml}$ ) for 36 hours. ....	14
Figure 2.3. Cell Proliferation Assay (PrestoBlue) of hMSCs after incubating with SPIO (labeled with media containing Fe: 0 $\mu\text{g}/\text{ml}$ , 50 $\mu\text{g}/\text{ml}$ , 100 $\mu\text{g}/\text{ml}$ , and 200 $\mu\text{g}/\text{ml}$ ) for 48 hours.....	15
Figure 2.4. DiI labeled SPIOs inside the hMSC. Figure a. shows the DiI labeled SPIOs alone. Figure b. shows the cell nucleus labeled with Hoescht and Figure c. shows both cell nucleus and the particles inside the hMSCs .....	16
Figure 2.5. Flow Cytometry of the DiI labeled SPIOs inside the hMSC. Figure a. shows the hMSCs alone. Figure b. shows the hMSCs labeled with SPIOs.....	17
Figure 2.6. SPIO release out of hMSCs over 24 hour time period. The concentration of iron in the culture media was not increased significantly over time.....	18
Figure 2.7. T2 map of the SPIO delivered hMSCs embedded in 0.5% agarose gel. ....	19
Figure 2.8. The width of the Z-spectrum using CEST method. Contrast increases in a concentration dependent manner. From right to left, this indicates the uptake of SPIOs by the hMSC. ....	20
Figure 2.9. T2 Calculated Image of cells suspended in agarose gel. ....	21
Figure 3.1. Schematic of PET/MR contrast agent with $^{64}\text{Cu}$ chelated by 14-PE DTPA and SPIO. ....	23
Figure 3.2. PEG Density on the surface of the SPIOs. The loading ratio of PEG per iron was changed from 1 to 1 to 1 to 4.....	25

Figure 3.3. TLC result for Cu-64 SPIOs. The peak at 60 cm indicates there are free $^{64}\text{Cu}$ in the solution.....	27
Figure 3.4. TLC result for Cu-64 SPIOs after the first and second desalting. The graph on the left shows that after the second desalting all the free $^{64}\text{Cu}$ is removed and the solution only contains radiolabeled SPIOs. ....	28
Figure 3.5. TLC silicagel paper showing the location of the SPIO sample.....	29
Figure 3.6. TLC result for $^{64}\text{Cu}$ labeled SPIOs incubated in mouse serum for 3 hours with constant shaking.....	30
Figure 3.7. TLC result for Cu-64 SPIOs incubated in mouse serum for 24 hours with constant shaking.....	30

## NOMENCLATURE

1,2-distearoyl-sn-glycero-3-phosphoethanolamine- N-[methoxy(polyethylene glycol)]	(DSPEmPEG)
Chemical exchange saturation transfer	(CEST)
End stage renal disease	(ESRD)
Poly(ethylene glycol)	(PEG)
Radiochemical thin layer chromatography	(radio-TLC)
Radio chemical purity	(RCP)
Reticulou endothelial system	(RES)
Nephrogenic systemic fibrosis	(NSF)
Magnetic resonance	(MR)
Signal-to-noise ratio	(SNR)

## SUMMARY

Development of nanostructures as MR contrast agent will significantly improve the field of disease diagnostics. Contrast agents such as iron oxide nanoparticles are less toxic compared to more commonly used gadolinium based agents. A subclass of iron based nano particles are super paramagnetic iron oxide nano particles, (SPIOs) which are widely studied MR contrast agents useful in both imaging and drug delivery applications. In this work, SPIOs were synthesized and characterized and used for cellular tracking and multi modal labeling. A new solvent exchange method was utilized to coat different core size iron oxide nano particles. SPIOs were characterized for in-vivo imaging using MR and they had a very uniform size distribution which was determine using dynamic light scattering (DLS) and transmission electron microscopy. Furthermore, blood circulation half-life of 16nm SPIOs were determined through tail vein injection.

SPIOs have many applications among which is the in vivo tracking of stem cells which is critical for determination of stem cells fate after injection. Magnetic Resonance (MR) as a non-invasive method can provide significant information about the fate of the cells as well as determination of the success rate of therapeutic cellular deliveries. Mesenchymal stem cells can be loaded with super paramagnetic iron oxide nano particles (SPIOs) and have their movements followed once planted in vivo. We present our findings on the effect of SPIO concentration and stem cell density on the MR signal and transverse relaxation time. Our preliminary results indicated that SPIOs do not cause mesenchymal stem cell cytotoxicity and do not affect proliferation ability up to 200  $\mu\text{g/ml}$  concentration. The release of the nanoparticles was investigated 24 hours post



internalization and the result showed that SPIOs will stay inside the cell. We also found that the contrast increases in a concentration dependent manner. Our results suggest that using MR with low concentration of SPIOs is a novel and promising method for tracking of mesenchymal stem cells.

In this work SPIOs were also labeled with  $^{64}\text{Cu}$  to investigate their potential for multi modal positron emission tomography (PET) MR imaging. Dual modality PET MR SPIO contrast agent can be synthesized to image diseases such as cancer and atherosclerosis. The advantage is the non-invasive and early detection of disease at molecular level before it has spread to late stages or in case of the atherosclerosis before the plaque has blocked the vessel. To develop a multi modal contrast agent, a positron emitter,  $^{64}\text{Cu}$  (half-life of  $12.701 \pm 0.002$  hours), was used in labeling and synthesis was performed all in one step with the addition of  $^{64}\text{Cu}$  chelator, 14-PE DTPA followed by radiolabeling for both 6.5nm SPIO and 17nm SPIO. After labeling and purification with the desalting column, the amount of dissociated  $^{64}\text{Cu}$  in the solution was determined using radio thin layer chromatography (TLC) and the particle was shown to have minimum amount of free  $^{64}\text{Cu}$ . Serum stability of labeled SPIO was determined in vitro by incubating  $^{64}\text{Cu}$ -labeled SPIOs in mouse serum at  $37^\circ\text{C}$  for 24 hr with constant shaking. Radio TLC result then revealed that  $^{64}\text{Cu}$  stays bounded to the SPIO after 24 hours in mouse serum. This means that  $^{64}\text{Cu}$  labeled SPIO has a great potential as a dual modality contrast agents and further in-vivo studies are required to verify the findings.

## CHAPTER 1: SYNTHESIS AND CHARACTERIZATION OF SPIO

Development and characterization of a biocompatible magnetic resonance (MR) contrast agent with sufficient in vivo circulation half-life has been a challenge for many years. Among the currently existing MR contrast agents the most widely used in the clinic is the gadolinium(III) chelate commonly referred to as “gado”[1]. Although it is widely utilized and studied, it is believed that it may cause nephrogenic systemic fibrosis (NSF) in patients with end stage renal disease (ESRD)[2, 3]. This can be prevented by using iron oxide based contrast agents such as super paramagnetic iron oxide nanoparticles.

MR imaging modality with its non-invasive methods is characterized by high resolution of soft-tissues without the dangers of radiation exposure. The signal intensity of MR imaging is determined, in part, by longitudinal relaxation time (T1) and transverse relaxation time (T2). Since MR imaging captures both healthy and pathological tissues, contrast agents such as paramagnet gadolinium are used to help visualize and distinguish between the two tissue types. However, some contrast agents are more effective in T1 while other contrast agents more effective in T2. For example, gadolinium contrast agents are T1 contrast agents since the percentage increase in  $1/T1$  in tissue is much greater than  $1/T2$  [1].

Iron contrast agents are also used in MR imaging and are best visualized with T2 weighted scans. Super paramagnetic iron oxide nano particles, (SPIOs) are widely studied MR contrast agents useful in both imaging and drug delivery applications. SPIOs have two basic components: (1) the core which is made of inverse spinel crystal Magnetite ( $Fe_3O_4$ ) and Maghemite ( $\gamma Fe_2O_3$ ); and, (2) the coating which is used to

increase the circulation half-life of the SPIO and to also make them biocompatible for in vivo applications. In our lab the iron oxide cores were coated with polymers such as poly(ethylene glycol) PEG. The two materials making up the core of SPIO are similar in crystal structure but Maghemite has lower saturation magnetization.

Maghemite and magnetite crystal, which make up the core of the SPIOs, are the major factor in signal enhancement of these nano particles. The core crystal of SPIOs has unpaired electron pairs which align to give rise to the magnetic properties of the nanoparticle. Furthermore, the magnetite crystal at nanometer scale has single crystal domain that cause them to exhibit superparamagnetic behavior.

SPIOs can be loaded with reporter molecules such as radionuclide and targeting proteins and peptides. In our lab, we have developed a new method for synthesizing SPIOs with tight control over their diameter and surface chemistry [4].

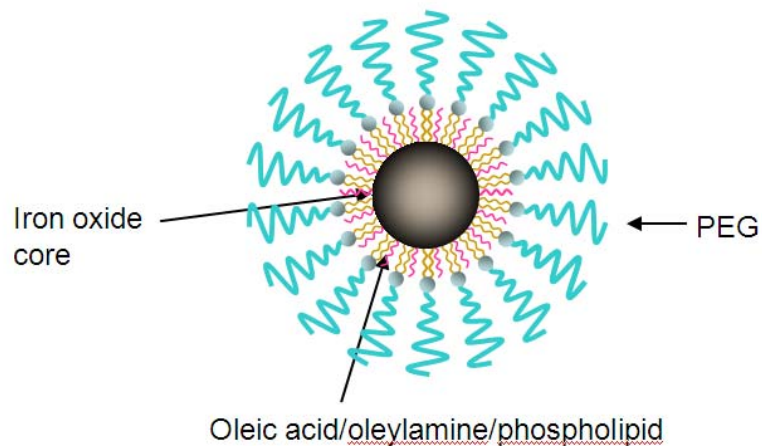


Figure 1.1. Schematic diagram of SPIO structure. The core is made of iron oxide with a combined coating of Oleic acid and oleylamine. The final coating is made of PEG.

The significance of this new coating method is that it allows for the SPIOs to be functionalized for targeting and imaging purposes. Therefore, it is a better way to distinguish healthy from pathological tissue.

### **1.1 Developing SPIO as an MR contrast agent**

Iron oxide core of 16.5 average diameter was synthesized in our lab with a coating of oleic acid and oleic amine to stabilize the core. The thermal decomposition method which was used to make the core improves the size distribution of nanoparticles. Figure 1.2 shows a TEM image of the 16.5nm iron oxide cores synthesized. The core size of 16.5 nm was obtained by employing controllable crystallization through thermodecomposition of iron complex in organic solvents [5, 6].

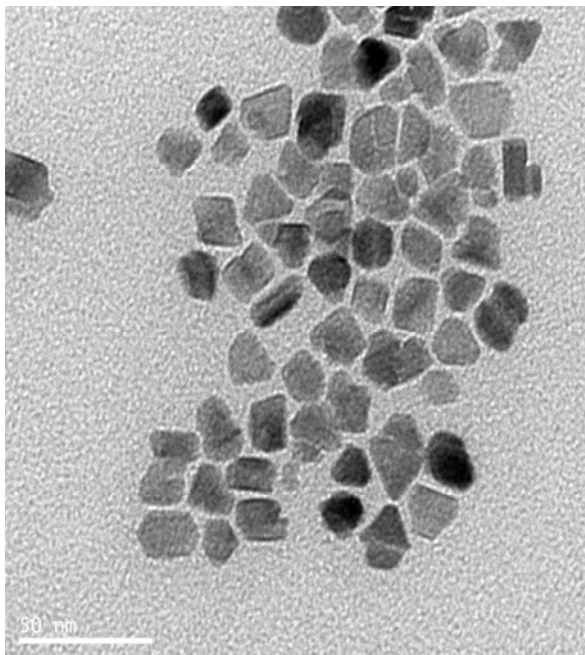


Figure 1.2. Iron Oxide Cores synthesized using thermodecomposition of iron complex in organic solvents

The cores were then coated with 1,2-distearoyl-sn-glycero-3-phosphoethanolamine-N-[methoxy(polyethylene glycol)] copolymer (DSPE-mPEG). A novel solvent-exchange method was developed in our lab in which DSPE-PEG and iron oxide nanocrystals assemble in a solvent system with ascending solvent polarity. This method yields high quality SPIOs with much improved coating efficiency and size distribution [7]. Figure 1.3 shows the TEM image of the coated SPIO. Images were obtained with JEOL JEM-1210 Transmission Electron Microscope.

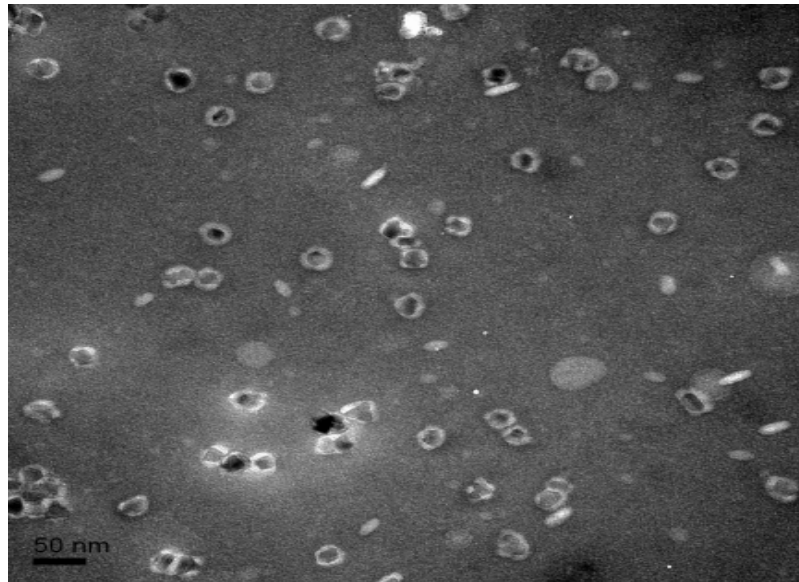


Figure 1.3. TEM images of the coated SPIO using the dual-exchange solvent method. SPIOs were negatively stained with phosphotungstic acid to show a white layer surrounding the iron oxide cores indicating the DSPE-mPEG2000 coating layer.

As it is shown in the image, the SPIOs are very uniform in size. The PEG coating can be clearly seen as a white layer surrounding the iron oxide core. This coating was performed with a 1 to 2 weight ratio of PEG to iron.

## 1.2 Particle Characterization

After the synthesis of any type of nano-structure, it is crucial to characterize it. The size distribution of the SPIOs was determined using DLS and TEM imaging. This ensured that the particle population was uniform. The T2 relaxivity was then determined using a Bruker minispec T2 analyzer. Circulation half-life was also determined by intravenous injection of Balb/C mice.

## 1.3 Particle Size

The size distribution of the SPIOs were determined using a DynaPro DLS (dynamic light scattering) instrument. Figure 1.4 shows the DLS result for 16.5nm cores and the SPIOs coated with DSPE-mPEG2000. As it is shown by the red curve, after coating, the average size increased to 30.8 nm. Experiments reported here were performed with 200-fold averaging and a 40-s integration time. The laser power was adjusted so that all the samples gave scattering amplitude of  $\sim 10^6$  counts  $s^{-1}$ . The temperature was set at 25 °C.

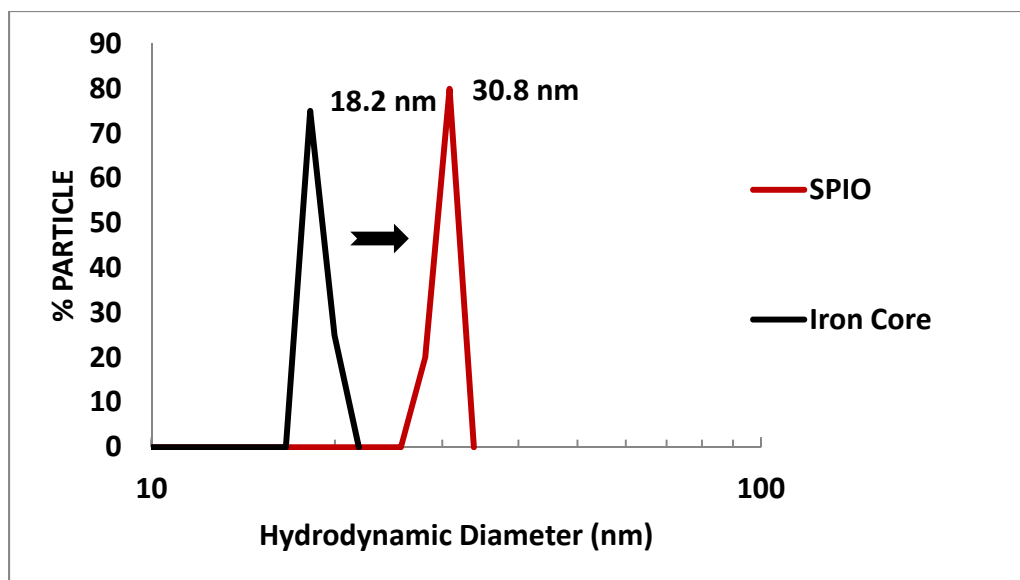


Figure 1.4. Size distribution of iron core and coated SPIO using a DynaPro NanoStar Dynamic Light Scattering Instrument

The differences in signal intensities among tissues with intrinsically different relaxation parameters are the basis for MR imaging. The presence of magnetic nano particles disturbs the magnetic field homogeneity and enhances tissue T2 relaxation. SPIOs are negative contrast agent as they make the tissue or sample containing them darker by decreasing the T2.

The T2 relaxivity (defined as  $1/T_2$  normalized by molar concentration of Fe atoms) of the SPIOs were measured with two core sizes (6.5 nm and 14 nm) and DSPE- PEG 2000 at 40 °C. The T2 relaxivity for 14 nm was  $184 \text{ s}^{-1} \text{ mM}^{-1} \text{ Fe}$  and decreased to  $114 \text{ s}^{-1} \text{ mM}^{-1} \text{ Fe}$  for the 6.5 nm core. Due to increased mass magnetization and core size, the 14 nm SPIOs consistently showed higher T2 relaxivity than the 6.5 nm SPIOs with the same coating. Using a larger core size particles, therefore, will yield better results when used for MR imaging purposes.

## 1.4 Circulation Half-life

Since the SPIOs are developed to be injected in-vivo they need to have a long blood circulation half-life so they can create a contrast. Circulation half life is an important parameter as the particle needs to be retained in the blood for a period of time to allow for imaging and accumulation of enough SPIOs inside the organ of interest. One way of improving the half life is through surface chemistry which has a strong influence on how long the particle circulates in the blood. The SPIOs are known to primarily clear out of circulation due to the phagocytosis of RES (Reticulo Endothelial System) in the liver and spleen. Micrometer sized constructs are cleared immediately following intravenous injection, however, pegylated nanoparticles such as SPIOs will have a much longer circulation in the blood[8-10]. Poly Ethylene Glycol (PEG) is an FDA approved coating which is used in our coating to reduce the affinity for the RES and improve stability. This will slow the uptake pathway and improve blood circulation half life. To determine blood circulation half-life, 0.05ml of 16nm core SPIO at a concentration of 1 mg/ml was injected through the tail vein in 2 Balb/C mice. Blood was drawn by tail nicking at 5min, 30min, 60 min, 120min, 180 min and 240 min. Figure 1.5 shows the corresponding data. The initial time data point on the graph is calculated based on the known weight of the mouse and the assumption that blood volume is 8% of the mouse body weight.



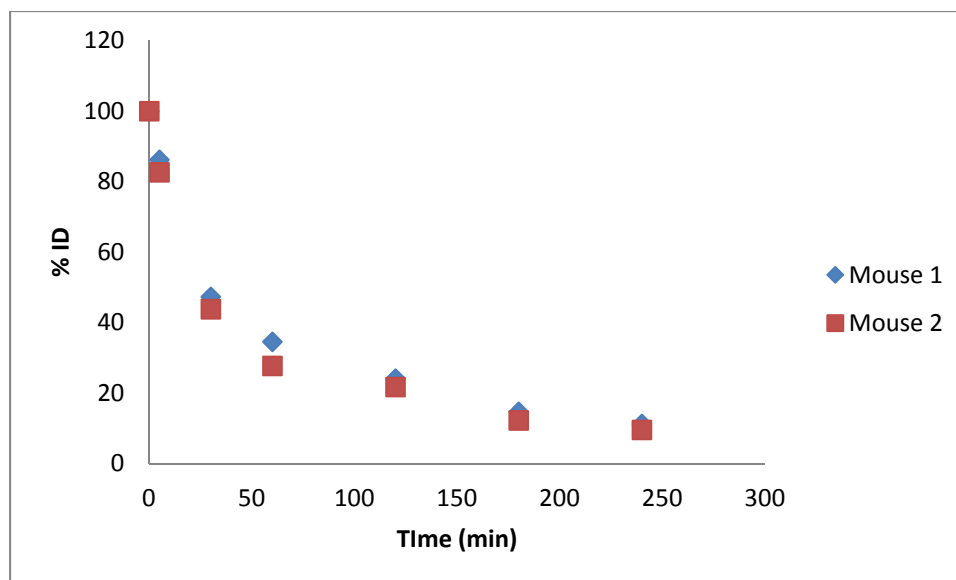


Figure 1.5. Blood clearance of 17nm SPIOs after intravenous injection. Blood samples were collected by tail nicking at 5, 30, 60, 120, 180 and 240 minutes post injection of SPIO. Amount of iron in the blood was quantified with a Ferrozine Assay. Data is shown as percent injected dose.

Based on the data shown in Figure 1.5, it was determined that the blood circulation half life of the 17nm SPIOs was 29.36 minutes. Therefore, the addition of the PEG on the surface of the SPIOs can significantly increase their circulation half life. PEG is believed to decrease RES uptake of the SPIOs by increasing the hydrophilicity of the SPIO's surface. This will reduce the non-specific interaction of SPIOs with RES cells in vivo. To see the effect of SPIO core size on blood circulation half, 6.5nm and 14 nm core size SPIOs were coated with PEG 2000. Intravenous injection of 0.15 ml of 1mg/ml SPIOs were performed on two Balb/C mice. Blood circulation half-life of 14 nm SPIO was only about 15 minutes and that of 6nm SPIO was 40 minutes.

## CHAPTER 2: STEM CELL TRACKING

### 2.1 INTRODUCTION

Nano particles can be loaded to cells of many type ex-vivo in order to track their movement once implanted. Traditional methods of cell tracking includes the use of invasive chamber models with intravital microscopy [11] or using flow cytometry of the fluorescently labeled cells from excised tissues [12]. In-vivo MR tracking of cells can provide valuable information and be useful in the fields of cancer therapy, cardiovascular disease, and neuro-imaging. Stem cells can be loaded with SPIOs and have their movement followed once planted in vivo. MR tracking of the cells is a non-invasive method to determine the success rate of therapeutic cellular deliveries. Stem cells migration and dynamics within individual animal model can be observed with high resolution MRI for a long period of time [13]. SPIOs are also used to track cells used for stem cell therapy and monitoring the fate of dendritic cells administered as a cancer vaccine. Since cells do not always localize in the target organ once delivered, in vivo MR tracking of these cells will allow for the better therapeutic design and administration of these cell based therapies. Simple incubation with SPIO can label many types of cells including monocytes and macrophages [14].

Smaller concentration of SPIO can produce MRI contrast compared to gadolinium contrast agents. Toxicity is also less of the problem since there is iron already present in the body and SPIOs can be naturally recycled after imaging is performed. It is however important to determine the sensitivity of the MRI signal to SPIO and also determine the minimum number of cells required in order to obtain a good signal.

Lewin and colleagues reported the observation of single cell in tissue samples using magnetic nanoparticles[15]. Progenitor cells have been tracked in vivo using Tat peptide-derived magnetic nanoparticles. The nanoparticle consist of a crosslinked (CL) dextran coated 5nm iron oxide core. The dextran coating was also reacted with DTPA to allow labeling with <sup>111</sup>In used for nuclear imaging. The achieved labeling efficiencies for the different cells ranging from 10 to 30 pg of superparamagnetic iron per cell equivalent of up to 0.5- 2 x 10<sup>7</sup> nanoparticles/cell [15].

Heymer and colleagues used very small superparamagnetic iron oxide particles (VSOPs). They observed the endocytosis in human mesenchymal stem cells using histology and quantified the amount of iron uptake by mass spectrometry. It was also found that cell viability and proliferation potential of the cells was not affected when compared with unlabelled cells [16].

## **2.2 SPIO DELIVERY**

The adherent hMSCs were cultured in MEA-Alpha supplemented with Gentamycin at 12.5 mg per 500 ml, 10% FBS, and 200mM L-Glutamine in a humidified 5% CO<sub>2</sub> atmosphere at 37 °C in 75 cm<sup>2</sup> flasks. A study was performed to determine the optimal time of incubation and concentration of hMSCs labeled with SPIOs in vitro. To treat the cells with the nanoparticles, 50,000 cells per well were seeded into 24-well plate for iron content measurement. The cells were cultured for 24 h, and then the media containing different concentrations of the nanoparticles were exchanged into wells, and cells were cultured for more various times.

### 2.3 Measurement of Cell Iron Content

Human Mesenchymal Stem Cell line was then cultured with different concentration of 16.5nm core size SPIO and different time of incubation (labeled with media containing Fe: 50 µg/ml, and 100 µg/ml and for 1hour, 3hr, 24hour). The amount of SPIOs in cells was quantified by using a Ferrozine Assay developed in our lab. After the treatment with 16.5nm SPIOs, cells were washed three times with PBS, collected in a 1.5-mL tube, and counted using hemacytometer. Cell solutions were then precipitated by centrifugation, resuspended in 50 µL of culture media. The cells were treated with 50 µL of hydrochloric acid, and incubated at 37 °C for 1 h. To neutralize the acid, 240 µL of 2N NaOH was then added, followed by 50 µL of 4N AA, and 110 µL of 5% HH. The solution was centrifuged for 15min at 22000 g, and 50 µL of the supernatant was removed and mixed with 50 µL of Ferrozine or color solution in the well in the NUNC 384 plate. The plate was read after 40 minutes using a Safire TECAN plate reader. A blank control cell sample was used to confirm the absence of iron contamination in the tested cells. The average iron content per cell was calculated by dividing the total iron content of the sample by the number of cells in the sample. The uptake of SPIOs was not significant within the first 3 hours at both 50 µg/ml and 100 µg/ml. The uptake was increased to 15.5 pg/ml per cell for the 50 µg/ml and 17.6 pg for the 100 µg/ml. This agrees with previous reports by Weissleder group[17].

## 2.4 CYTOTOXICITY ASSAY

Although the iron oxide core of SPIO is harmless at low doses and the PEG coating is biocompatible, before injecting hMSCs with SPIO and performing in-vivo studies it is important to determine the cytotoxicity and cell viability after a long incubation time[18]. Therefore, after delivering SPIOs to the hMSCs, their viability was determined using trypan blue staining. Equal volume of Trypan blue and cell solutions were incubated for 10 minutes. The number of unstained (viable) and stained (nonviable) cells were counted separately in the hemacytometer. To obtain the total number of viable cells per ml of aliquot, the total number of viable cells was multiplied by 2 (the dilution factor for trypan blue). To obtain the total number of cells per ml of aliquot, the total number of viable and nonviable cells was add up and multiplied by 2. The percentage of viable cells was then calculated as follows:

$$\text{viable cells (\%)} = \frac{\text{Total number of viable cells per ml of aliquot}}{\text{Total number of cells per ml of aliquot}} \times 10$$

To see the effect of SPIOs on cell viability, hMSCs were incubated with different concentration of SPIO (labeled with media containing Fe: 0 µg /ml, 50 µg/ml, 100 µg/ml, and 200 µg/ml) for 24 and 36 hours. Figure 2.1 shows the result of the Trypan Blue viability assay on hMSCs after 24 hours incubation with SPIOs.

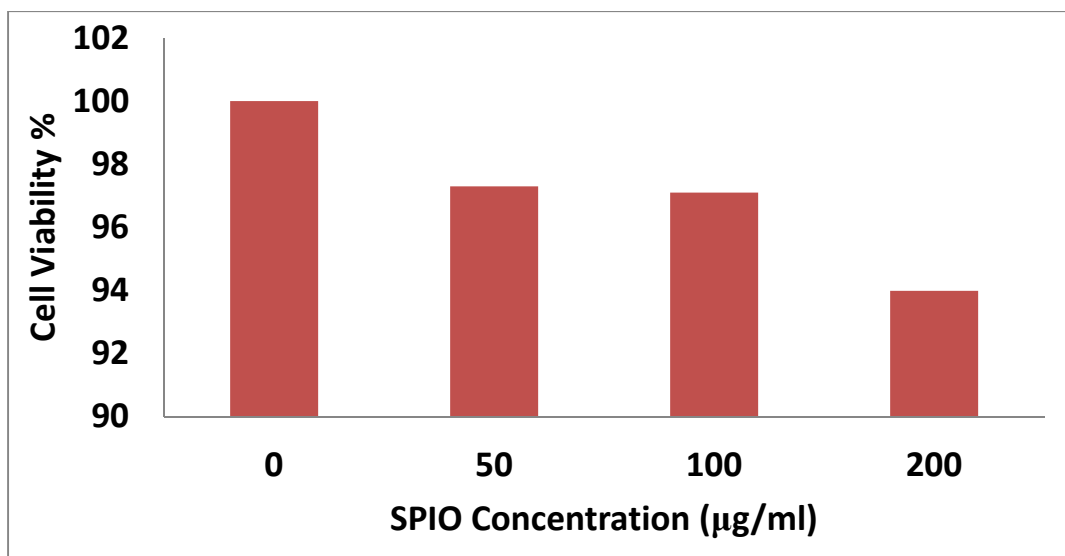


Figure 2.1. Cell Viability Assay of hMSCs after incubating with SPIO (labeled with media containing Fe: 0 µg /ml, 50 µg/ml, 100 µg/ml, and 200 µg/ml) for 24 hours

As it is shown in Figure 2.1, cell viability was not greatly affected at 50 µg/ml and 100 µg/ml concentration. Even at the 200 µg/ml concentration of Fe, the viability remained at 94% after 24 hour incubation.

Figure 2.2 shows the result of the Trypan Blue viability assay on hMSCs after 36 hours incubation with SPIOs. At 50 µg/ml and 100 µg/ml, toxicity was minimum and it increased to 6% at 200 µg/ml. This result agrees with the previously reported studies of SPIOs and their affect on cell viability.

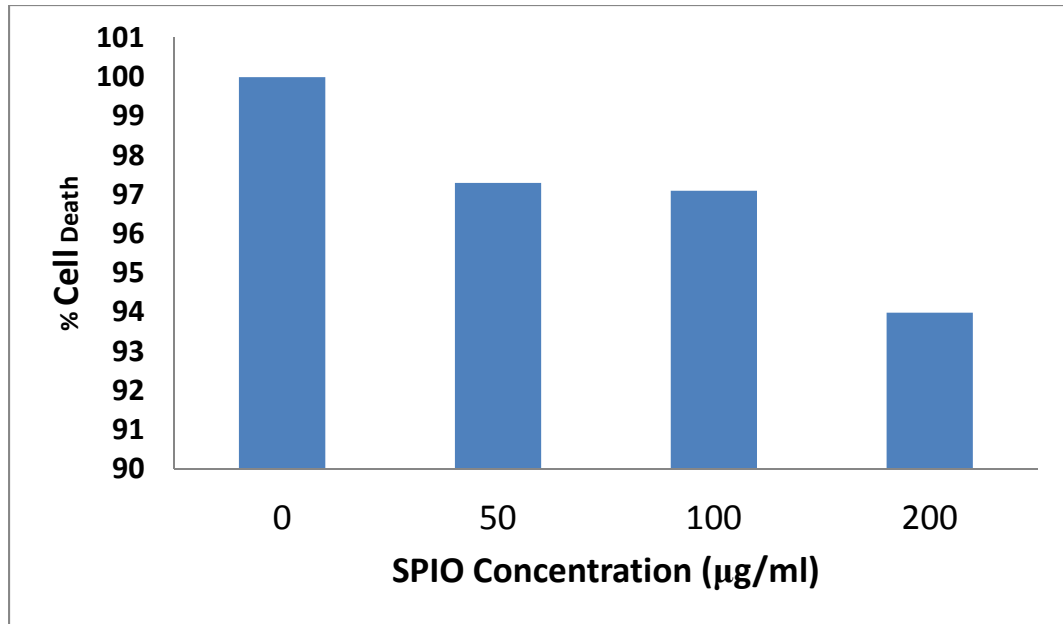


Figure 2.2. Cell Viability Assay of hMSCs after incubating with SPIO (labeled with media containing Fe: 0 µg /ml, 50 µg/ml, 100 µg/ml, and 200 µg/ml) for 36 hours.

Trypan Blue is a dye exclusion method but it is subject to the problem that viability is being determined indirectly from cell membrane integrity. Thus, it is possible that a cell's viability may have been compromised (as measured by capacity to grow or function) even though its membrane integrity is maintained. Therefore, it was necessary to also test cell proliferation and for that reason PrestoBlue cell proliferation assay was used to test the viability and proliferation of hMSCs incubated with SPIOs. This reagent uses the reducing power of living cells to quantitatively measure the proliferation of cells. Figure 2.3 shows the result of the PrestoBlue proliferation assay.

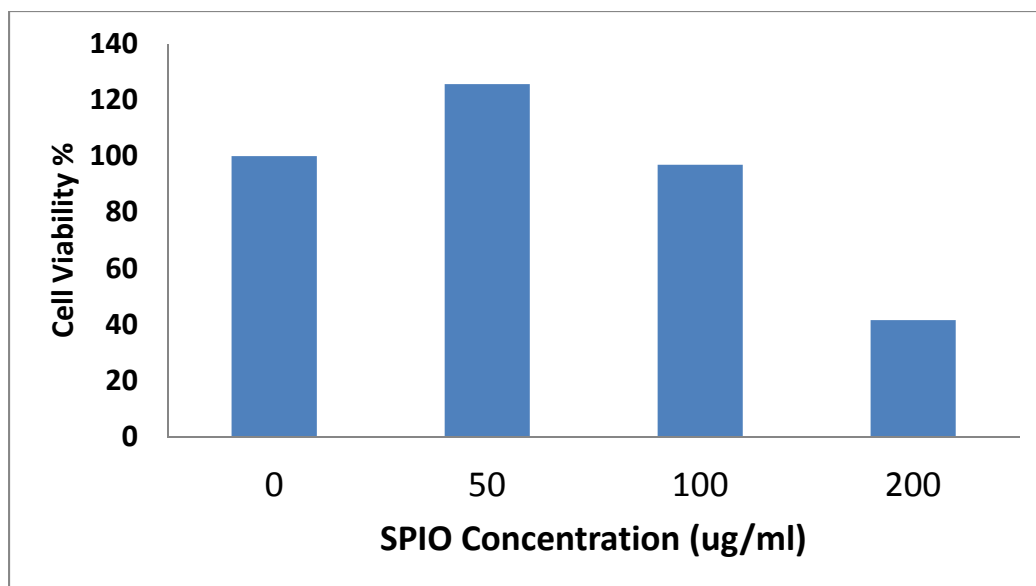


Figure 2.3. Cell Proliferation Assay (PrestoBlue) of hMSCs after incubating with SPIO (labeled with media containing Fe: 0  $\mu\text{g/ml}$ , 50  $\mu\text{g/ml}$ , 100  $\mu\text{g/ml}$ , and 200  $\mu\text{g/ml}$ ) for 48 hours

As it is shown cell proliferation was greatly affected by the high concentration at 200  $\mu\text{g/ml}$ . Based on this result it is best to either use the 50  $\mu\text{g/ml}$  or the 100  $\mu\text{g/ml}$  concentration. The amount of iron uptaken by the cells was quantified using Ferrozine colorimetric assay and it was found that after 24 hours, 15.5 pg of SPIO will be uptaken per cell. This agrees with previous reports.

## 2.5 CONFOCAL MICROSCOPY

To further investigate labeling efficiency and intracellular localization, several studies were performed with hMSCs. In this study, 100  $\mu\text{g/ml}$  of DiI labeled SPIOs were incubated with hMSCs for 24 hours. Cell nucleus was stained using Hoescht and confocal microscopy analysis confirmed that SPIOs were internalized into hMSCs. The particles were mainly localized into the cytoplasm as shown in figure 2.4.



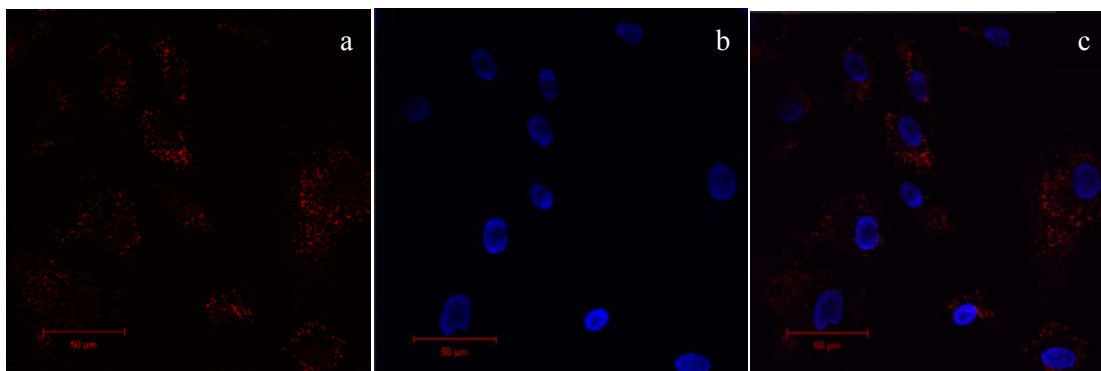


Figure 2.4. DiI labeled SPIOs inside the hMSC. Figure a. shows the DiI labeled SPIOs alone. Figure b. shows the cell nucleus labeled with Hoescht and Figure c. shows both cell nucleus and the particles inside the hMSCs.

Endocytosis is thought to be the main mechanism by which nanoparticles enter the cells. However, it is believed that nanoparticles will also get out of the cell through transcytosis.

Flow Cytometry was also performed with DiI labeled SPIOs which were internalized into hMSCs. Figure 2.5 shows the result of Flow Cytometry experiment.

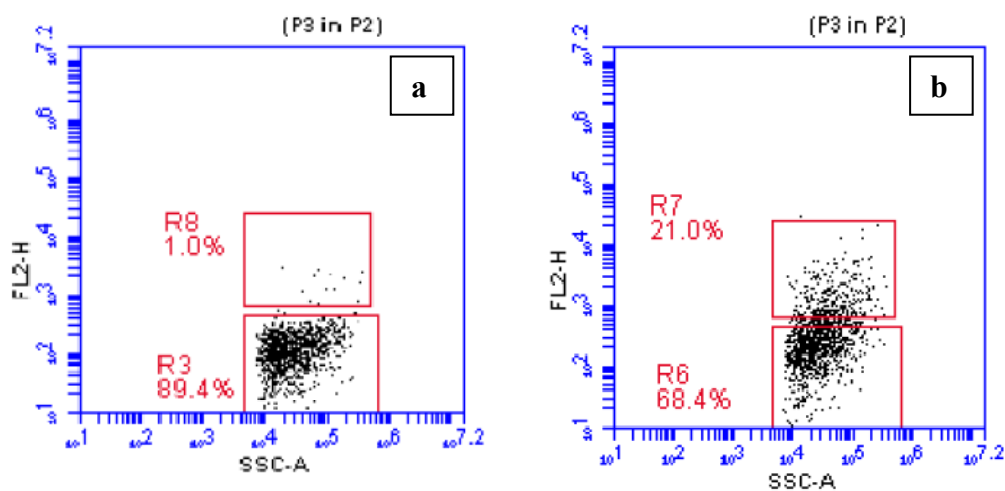


Figure 2.5. Flow Cytometry of the DiI labeled SPIOs inside the hMSC. Figure a. shows the hMSCs alone. Figure b. shows the hMSCs labeled with SPIOs.

Based on the confocal microscopy images and the flow cytometry data it was found that the SPIOs do indeed get internalized into the cell cytoplasm. The question is, however, if they get out of the cell once they are injected in vivo for imaging or therapeutic purposes. An experiment was designed to answer this question and also determine the rate at which SPIO get out of the hMSCs. The cells were incubated with 6nm SPIO for 1 hour on the magnet and the rest of the media containing nano particles was removed. The cells were washed with cold PBS three times to remove all the SPIOs that did not get internalized into the hMSCs. 2ml of Culture media was then added to the cells. A 50 ul sample of culture media was removed at times, 0, 1 hour, 3 hours, and 24 hours. At each time point Ferrozine Assay was used to determine the concentration of the SPIOs in the culture media. Cells incubated with culture media served as control in this study. Figure 2.6 shows the result of this experiment.

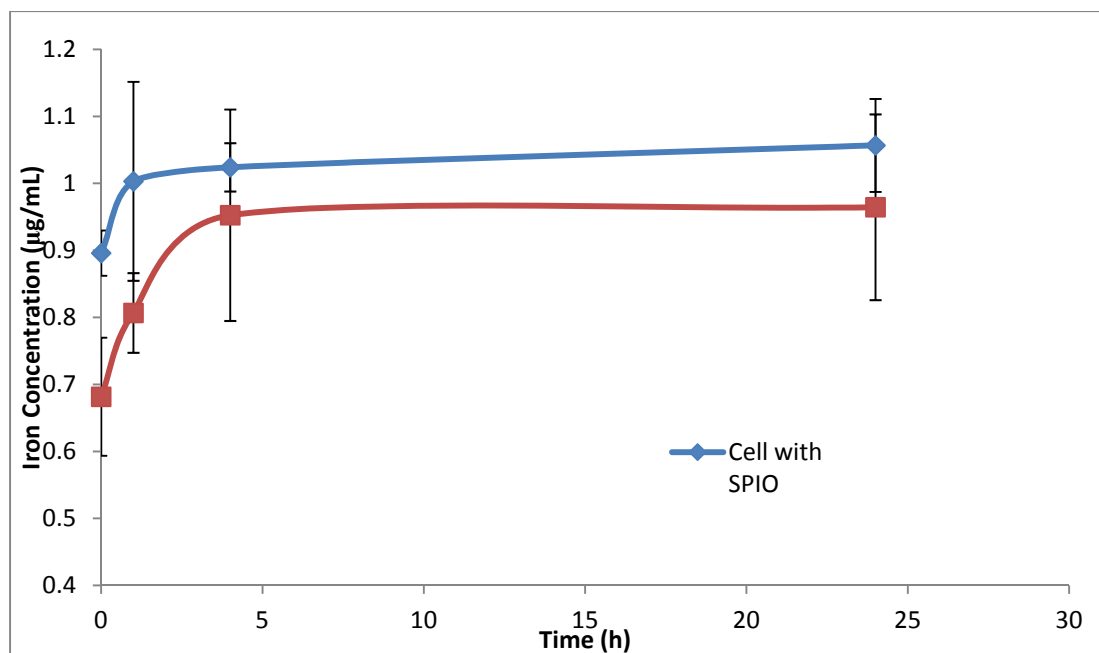


Figure 2.6. SPIO release out of hMSCs over 24 hour time period. The concentration of iron in the culture media was not increased significantly over time.

As shown in Figure 2.6, it was found that the amount of SPIO released from hMSCs is negligible. Data shows that the slight increase in iron concentration could be due to the endogenous iron as shown in the red control curve.

## 2.6 MRI of hMSCs

To determine the detection efficiency of MRI the 14.5nm SPIOs were incubated with hMSCs on the magnet at a concentration of 100 µg/ml for 1hour. After delivery, the Cells were washed with cold PBS three time, then trypsinized. The final sample contained 30ul of cell sample suspended into 30 ul of the 1% agarose gel. The wells were imaged with a 7T Bruker small animal MRI using a spin-echo sequence. The result is shown in Figure 2.7. The T2 map shows that the increase in concentration of the SPIO from 0 µg/ml to 100 µg/ml, also decreases the T2 for the same number of cells. It is also

observed that for the same concentration of the SPIO, T2 decreases as the number of cells increases from 2K to 14K.

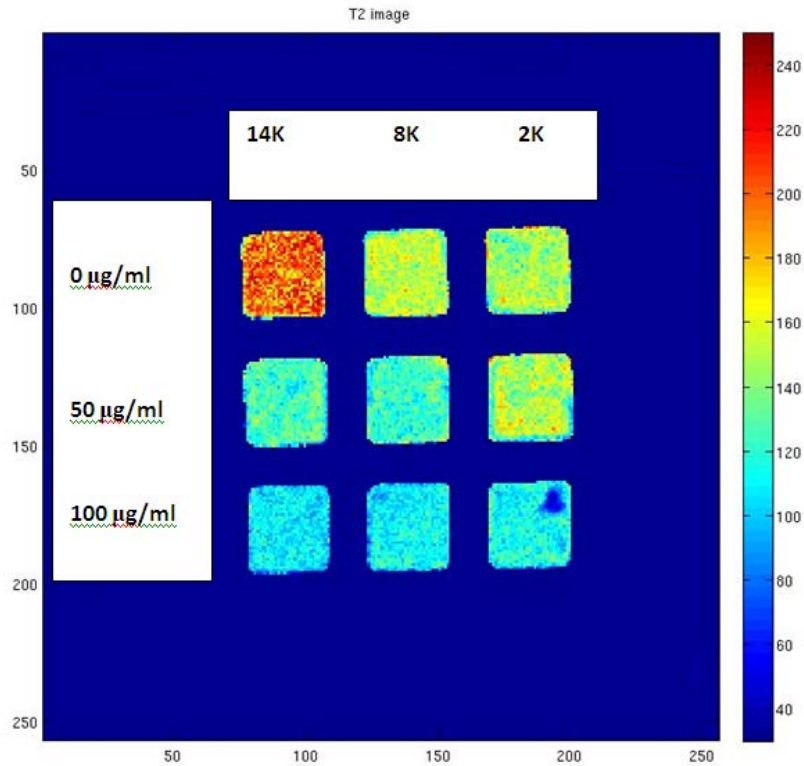


Figure 2.7. T2 map of the SPIO delivered hMSCs embedded in 0.5% agarose gel.

Chemical Exchange Saturation Transfer (CEST) is an MRI molecular imaging tool that helps resolve different signals arising from protons on different molecules. The location of the CEST agent can be revealed by saturating a particular proton signal that is in exchange with surrounding water molecules. Figure 2.8 shows the width of the z spectrum of the CEST image of the cells embedded in 1% agarose gel.

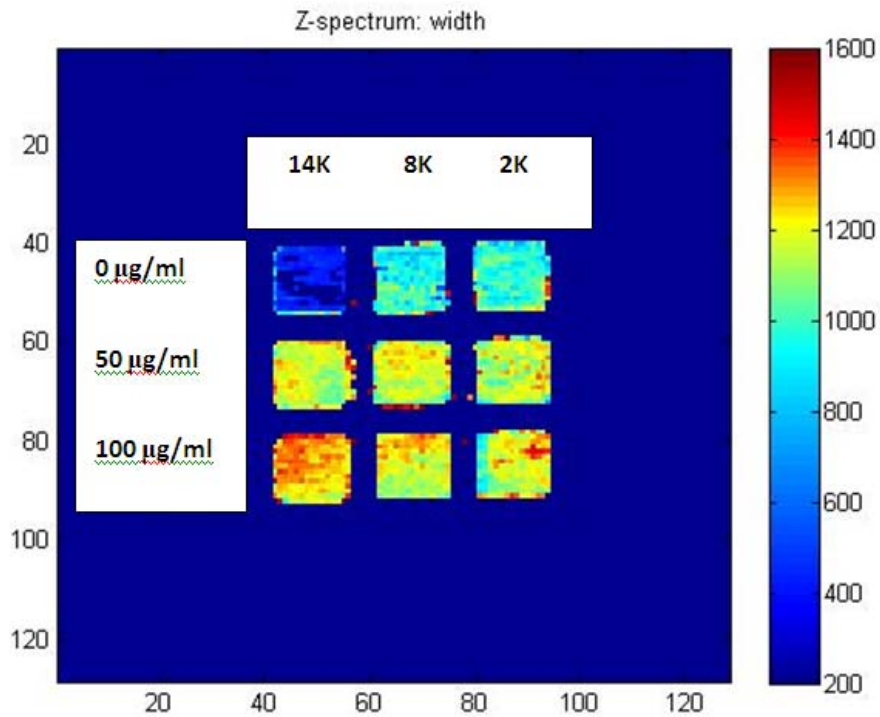


Figure 2.8. The width of the Z-spectrum using CEST method. Contrast increases in a concentration dependent manner. From right to left, this indicates the uptake of SPIOs by the hMSC.

The width of the Z-spectrum is correlated with the concentration of the SPIOs. As it is shown, the highest concentration of the SPIO is at the well with 14k cells and the initial concentration of 100ug/ml. The effect of increasing cell density is clearly observed for the 100 ug/ml row. As the cell density increases the width of the Z-spectrum also increases indicating an increase in SPIO concentration.

To observe and understand the effect of cell density and SPIO concentration on the MRI images, T2 was calculated and it is shown if Figure 2.9.

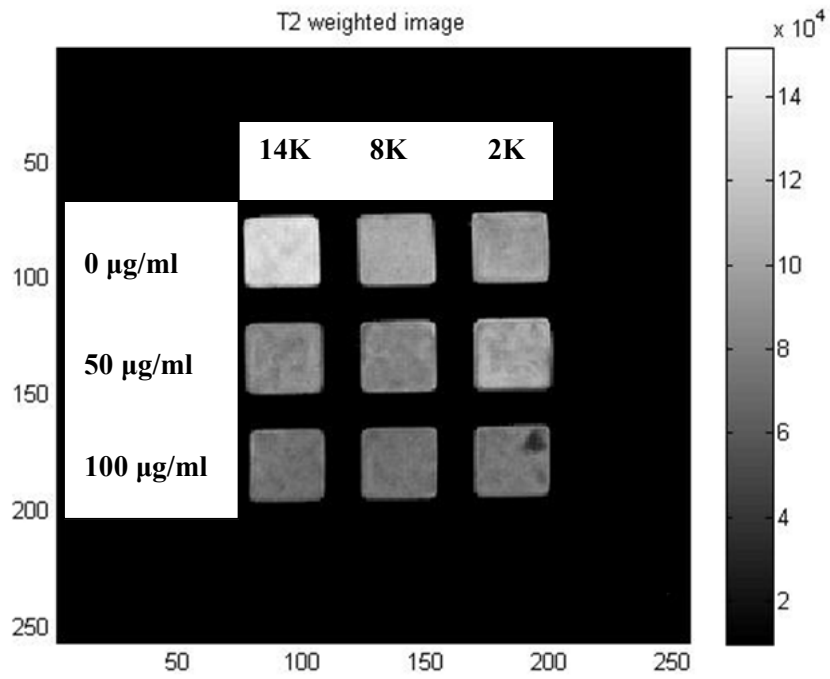


Figure 2.9. T2 Calculated Image of cells suspended in agarose gel.

The result demonstrates that the 14.5 nm SPIO labeled hMSC can affect the T2. Only 2000 SPIO labeled cells are enough to shorten the T2 as compared to the non-labeled cells.

### CHAPTER 3: DUAL MODALITY PET/MR CONTRAST AGENT

Positron Emission Tomography (PET) was created in 1970s to combine early biochemical assessment of pathology with the precise localization through the use of nuclear medicine and computerized image reconstruction. In this technique a biologically active chemical compound is labeled with a radioactive isotope that decays by emitting a positron. The positron then travels a small distance before combining with an electron and emitting two back to back gamma photons [19]. This technology has a very high sensitivity compared to other image modalities and PET images can be interpreted to provide regional assessment of biochemical processes. The lack of anatomical information was solved by combining PET with high resolution anatomical imaging like Computed Tomography (CT) in the late 1990s [20]. However, increased use of the CT which is associated with ionizing radiation has led to concern among the radiology community (radiologists, medical physicists, and manufacturers) [21]. Combination of PET and MR is an attractive option since MR provides high anatomical resolution without the harmful effects of ionizing radiation and much effort has been invested in developing a PET/MR diagnostic imaging system [22, 23]. To better visualize the existence of malignancy with this system, a dual modality contrast agent such as radio-labeled SPIO is developed. Dual modality PET MR SPIO contrast agent can be synthesized to image diseases such as cancer and atherosclerosis. The advantage is the non-invasive and early detection of disease at molecular level before it has spread to late stages or in case of the atherosclerosis before the plaque has blocked the vessel. There are however many challenges in the development of the multi-modal PET MR contrast agent.

The radionuclide used for PET imaging has a limited half-life; also chemical conjugation methodologies must be developed to ensure that the particle stays intact after it is exposed to the harsh environment inside the body [24].

The unique decay properties of  $^{64}\text{Cu}$  make it useful as a radiotracer for PET. It has a longer half life ( $12.701 \pm 0.002$  hours) compared to FDA approved  $^{18}\text{F}$  and decays by 17.86% positron emission, 39.0% by beta decay, 43.075% by electron capture and 0.475% gamma radiation/internal conversion. It can also be produced in high yield and high specific activity which is required for in-vivo PET imaging [25].

Figure 3.1 shows the schematic of PET/MR SPIO. The chelator 14-PE DTPA will not dissociate due to the strong hydrophobic interaction between the PEG chain and the 14 carbon chain of the chelator.

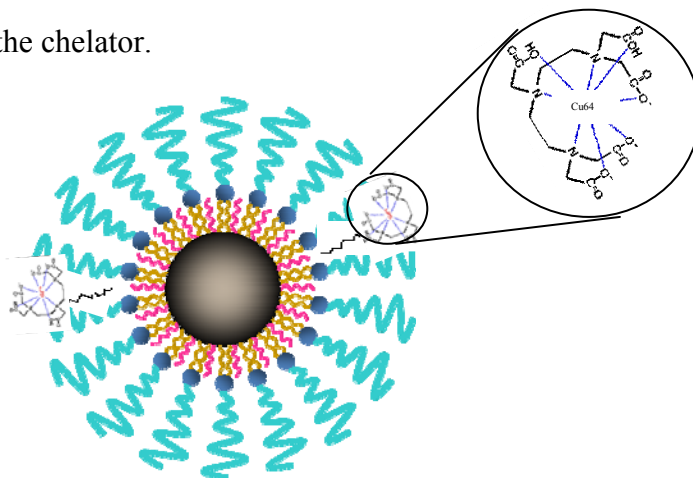


Figure 3.1. Schematic of PET/MR contrast agent with  $^{64}\text{Cu}$  chelated by 14-PE DTPA and SPIO.

### 3.1 Dual Modality Nanoparticles for PET MR Imaging

Jarrett et al has recently reported on a dual modality contrast agent made of  $^{64}\text{Cu}$  labeled dextran sulfate coated iron oxide nanoparticles. These nanoparticles were targeted to macrophages and tested in three different mouse and rat models of atherosclerosis. The



chelator DOTA was used to attach  $^{64}\text{Cu}$  to the particle and nanoparticles were purified by size exclusion chromatography (SEC) to yield CLIO-DOTA ( $^{64}\text{Cu}$ ). Separate PET and MR images were obtained 24 hours after contrast agent injection on ApoE<sup>-/-</sup> mice. The images were then coregistered and the three-dimensional volumes corresponding to probe uptake were traced and it was observed that the MR signal intensity was decreased. The contrast-to-noise ratio (CNR) at the aortic valve was increased by  $68\pm 10\%$  [26].

### 3.2 Synthesis of DTPA SPIO

Reactions were performed in oven-dried (140 °C) or flame-dried glassware under an atmosphere of dry air. Iron oxide cores were synthesized in the lab using a new method developed to control size and coating properties of the cores. Synthesis was performed using the novel solvent-exchanged method developed in our lab in which iron oxide nanocrystals were coated with 1,2-distearoyl-*sn*-glycero-3-phosphoethanolamine-N-[methoxy(polyethylene glycol)] copolymer (DSPEmPEG) and 1,2-ditetradecanoyl-*sn*-glycero-3-phosphoethanolamine-N-diethylenetriaminepentaacetic acid (DMPE-DTPA) at the same time. This method eliminates one step of the conjugation and the final product was then used in radio-labeling.

Before the start of the synthesis it was necessary to determine the amount of DMPE-DTPA required for the particle to have at least an average of 30 chelator per particle. Assuming 50% efficiency in radio-labeling, on average 15  $^{64}\text{Cu}$  per particle is necessary to produce a good PET signal. Therefore, a Malachite Green Phosphate detection kit was used to quantify the amount of DSPE-mPEG density on the surface of SPIOs. This assay will measure the phosphate concentration which will be correlated to amount of PEG on the surface of the nanoparticle since each DSPE-mPEG contains a phosphate group.

Aliquots of 100  $\mu\text{l}$  SPIO solutions were evaporated under vacuum and 500  $\mu\text{l}$  of 70% perchloric acid was added to each sample and the mixture was heated at 160°C for 20 minutes in an oil bath. 580  $\mu\text{l}$  of 10 M NaOH solution was then added to neutralize the pH. The concentration of phosphate in the solution was quantified with a Malachite green phosphate detection kit (R&D Systems). The assay was validated with solutions containing known amount of DSPE-mPEG. The result is shown in Figure 3.2.

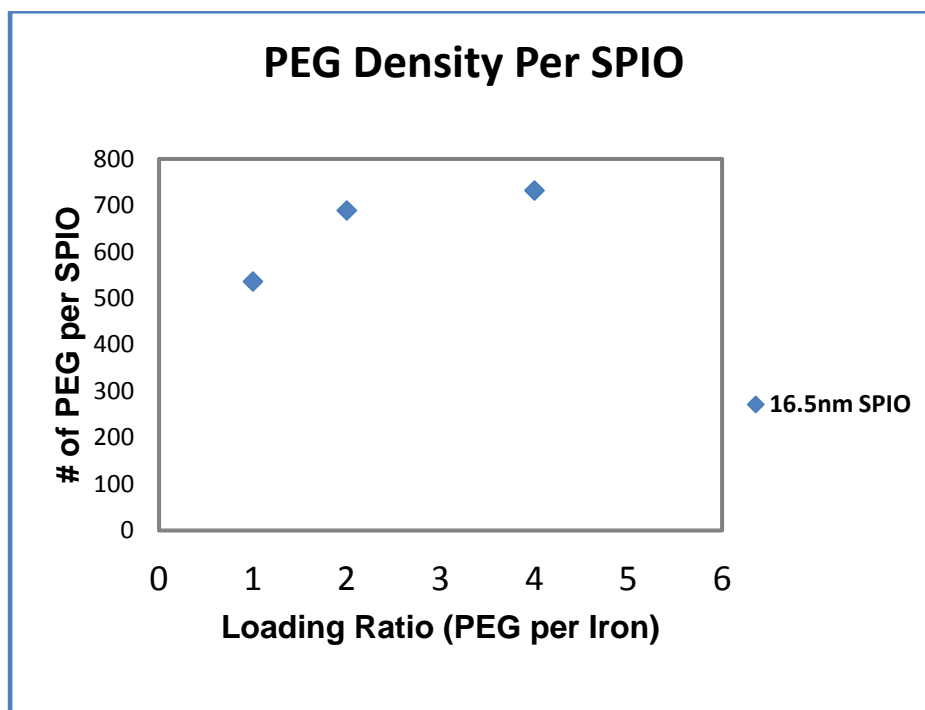


Figure 3.2. PEG Density on the surface of the SPIOs. The loading ratio of PEG per iron was changed from 1 to 1 to 1 to 4.

As it is shown the number of PEG per SPIO increased by increasing the loading ratio.

Based on this data the optimal ratio of DTPA to PEG was determined to be 5%.

### **3.3 Radiolabeling of DTPA SPIO with $^{64}\text{Cu}$**

Radiolabeling was performed for both 6.5nm SPIO and 17nm SPIO. DTPA SPIOs (0.25 mg in 250  $\mu\text{L}$ ) were incubated with  $^{64}\text{CuCl}_2$  (1.75 mCi in 2.2  $\mu\text{L}$ , 0.1 M HCl) in 0.1 M ammonium acetate buffer (pH 5.5) at 37 °C for 1 hr in a thermomixer. A glass test tube was used for reaction vessel. The temperature of the thermo mixer was stabilized one day before the experiment. Then 5  $\mu\text{L}$  of 10 mM EDTA was added into the solution and the mixture was placed in the thermo mixer at 37 °C for 5 min with mixing to remove nonspecifically bound  $^{64}\text{Cu}$ , followed by purification using a centrifugal desalting column (Pierce Biotechnology, Inc., Rockford, IL). To determine the amount of dissociated Cu-64 in the solution, TLC was performed before purifying with the desalting column. The result is shown in figure 3.3.

$^{64}\text{Cu}$ -SPIO

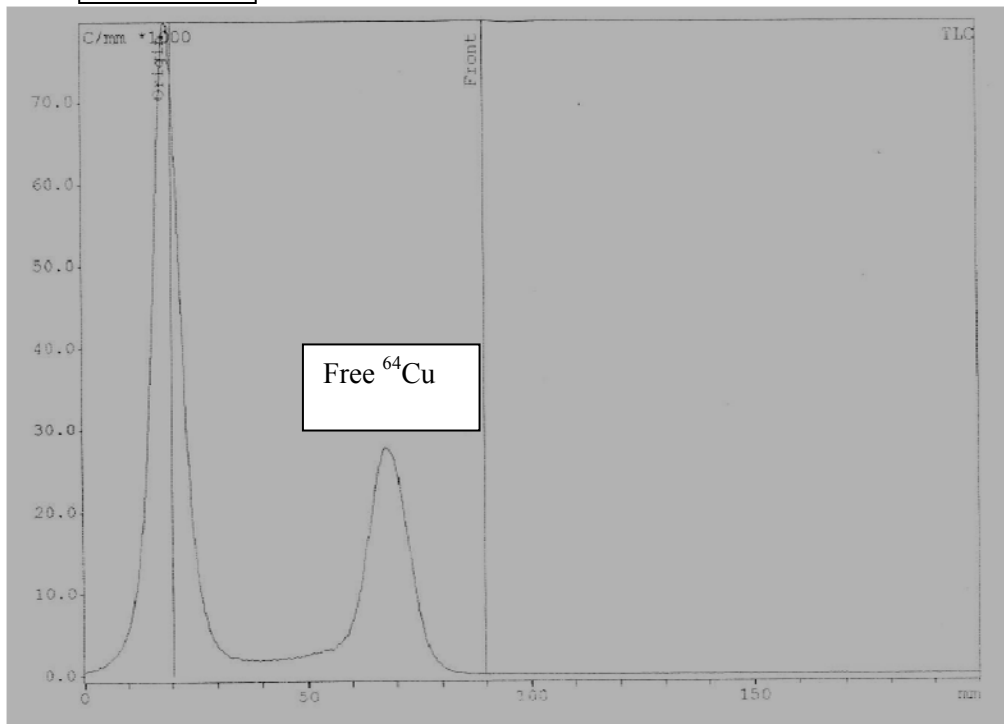


Figure 3.3. TLC result for Cu-64 SPIOs. The peak at 60 cm indicates there are free  $^{64}\text{Cu}$  in the solution.

Desalting column was used twice until all the free  $^{64}\text{Cu}$  was removed and the solution only contained radio-labeled SPIOs. The TLC result after the first and second desalting is shown in Figure 3.4.

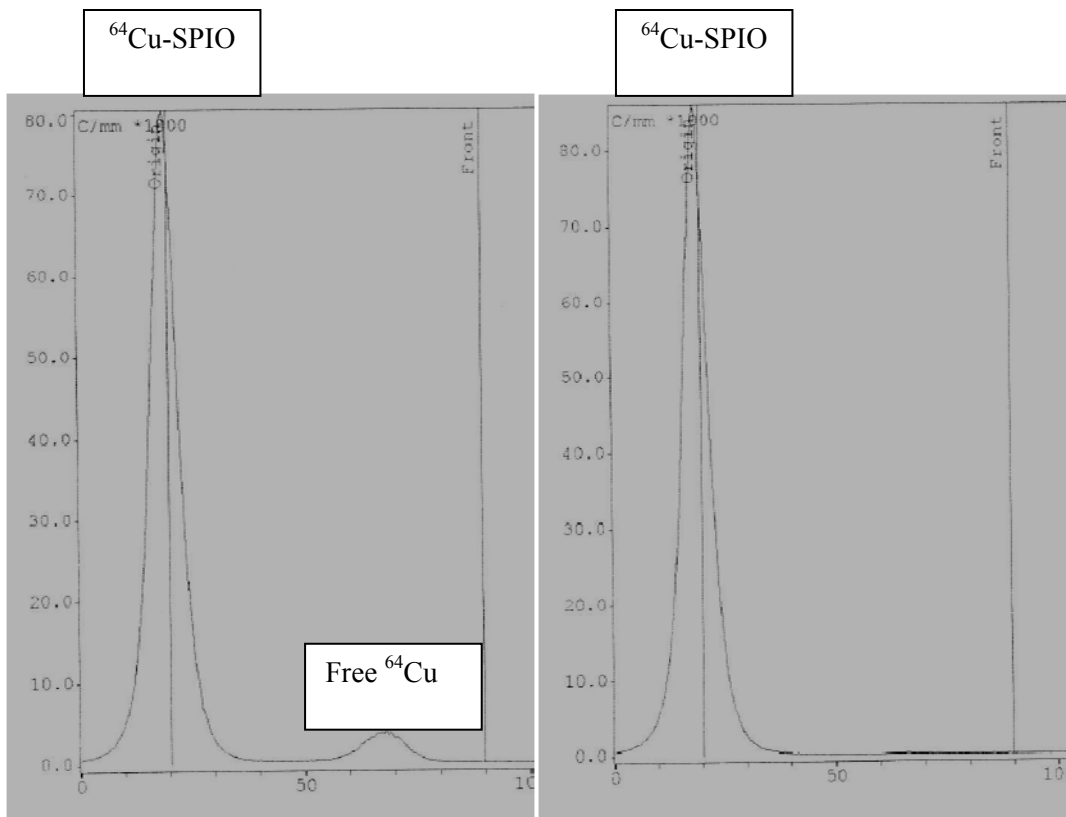


Figure 3.4. TLC result for Cu-64 SPIOs after the first and second desalting. The graph on the left shows that after the second desalting all the free  $^{64}\text{Cu}$  is removed and the solution only contains radiolabeled SPIOs.

Labeling yield was determined by radiochemical thin layer chromatography (radio-TLC). Figure 3.5 shows the TLC silicagel paper marked at the solvent front. A small amount of the of the  $^{64}\text{Cu}$  labeled SPIO solution was applied to an ITLC-SG plate (Pall Corporation, East Hills, NY) and developed using a 1/1 mixture (v/v) of ammonium acetate (10% w/v)/ methanol. The TLC plate is then measured using Raytest system (model Rita Star, Germany). Labeled  $^{64}\text{Cu}$  should stay at the spotting point ( $R_f = 0$ ) and the nonspecifically bound  $^{64}\text{Cu}$  should move to the top of the solvent front ( $R_f = 1$ ).

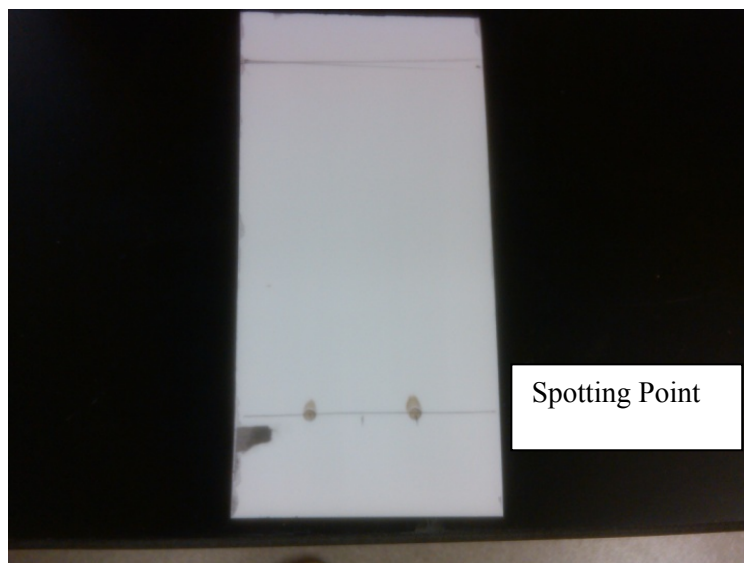


Figure 3.5. TLC silicagel paper showing the location of the SPIO sample.

### 3.4 Serum Stability of $^{64}\text{Cu}$ -labeled SPIO

Before injecting the  $^{64}\text{Cu}$ -labeled SPIO into the mice, it is necessary to determine the serum stability in vitro. This test was performed by incubating  $^{64}\text{Cu}$ -labeled SPIOs in mouse serum at 37 °C for 24 hr with constant shaking. The samples were then subjected to radio TLC analysis after 0, 1, 3, 6, and 24 hr incubation to measure the amount of activity dissociated from  $^{64}\text{Cu}$ -labeled SPIO. Figures 3.6 and 3.7 show the TLC results for the 16.5nm SPIO samples taken at 3 hours and 24 hours post incubation.

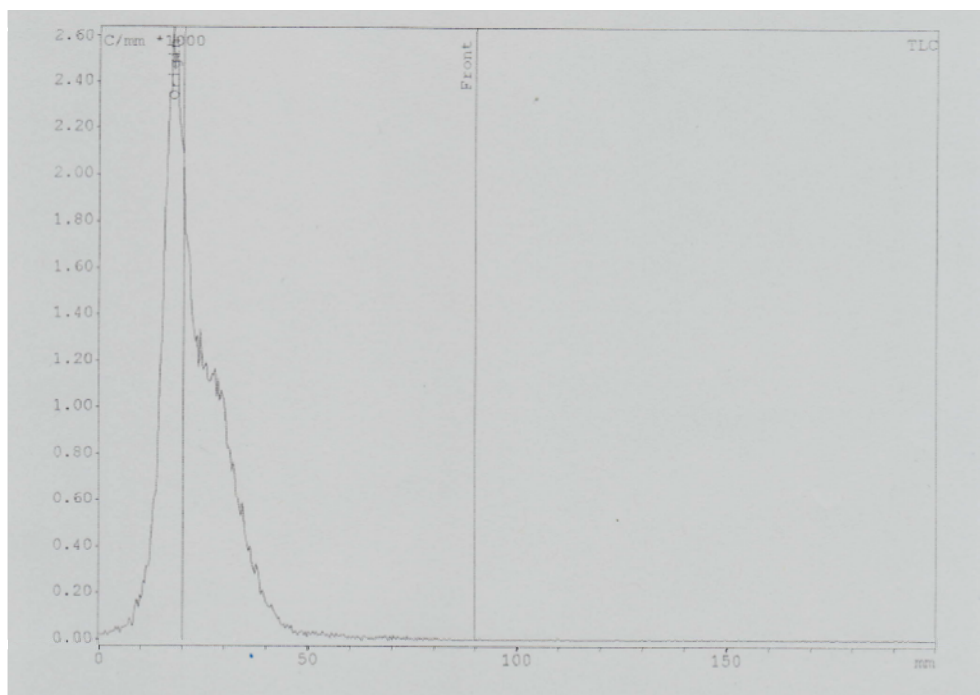


Figure 3.6. TLC result for  $^{64}\text{Cu}$  labeled SPIOs incubated in mouse serum for 3 hours with constant shaking.

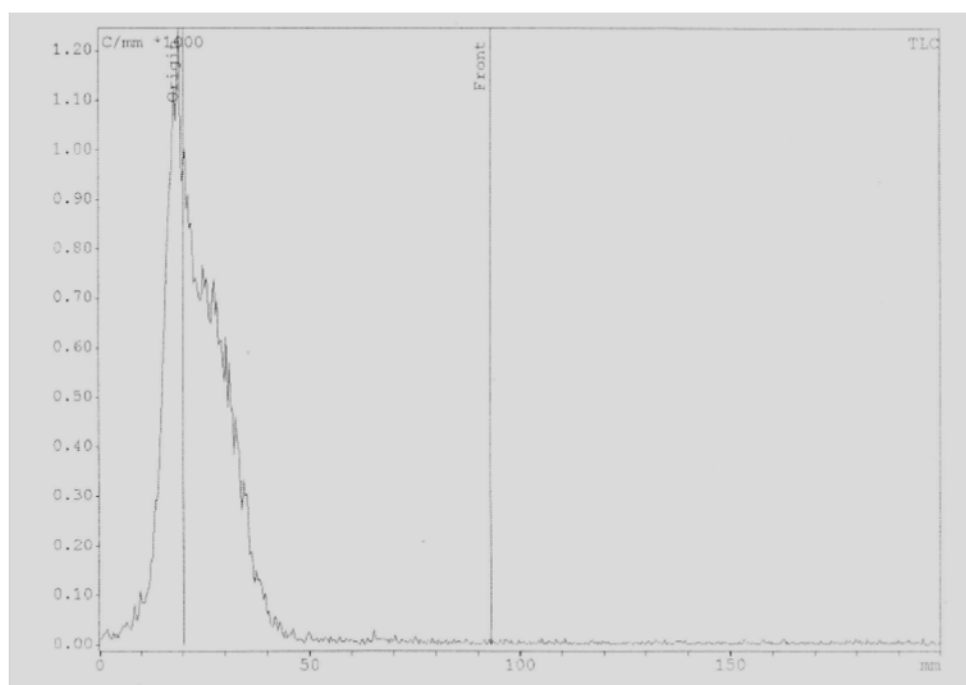


Figure 3.7. TLC result for Cu-64 SPIOs incubated in mouse serum for 24 hours with constant shaking.

Although there is no indication that there is free  $^{64}\text{Cu}$  dissociated from the SPIO in the mouse serum the result must be confirmed with FPLC system.



## CHAPTER 4: DISCUSSION, CONCLUSION AND FUTURE WORK

### 4.1 Discussion and Conclusion

The problem with all nano materials injected systematically is their relatively short circulation half life preventing long term imaging. To improve the circulation half life we coated our particles with PEG which is a synthetic hydrophilic polymer and serves as a barrier preventing interactions with plasma opsonins. We then compared the T2 relaxivity and circulation half life of 6.5 nm and 14 nm SPIOs to determine the best candidate for imaging. Based on the T2 relaxivity results, the large SPIOs will create higher contrast in MR and they have an advantage of higher surface to volume ratio. This means that they can be loaded with higher number of positron emitters which also yields better sensitivity in PET imaging. The disadvantage of using larger SPIO compared to the small one is their poor circulation half life however the time is still long enough to create contrast.

Our preliminary result of cellular studies indicates that SPIOs can be easily delivered into the cells and imaged with MRI. The concentration of 50 µg/ml is optimum for initial incubation and results in minimal toxicity to the cells. The minimum number of cells that were able to decrease the T2 time was 2000 hMSCs embedded in agarose gel. The noninvasive tracking of hMSCs to understand their distribution in-vivo will have significant impact on clinical imaging and therapeutic applications.

We were able to successfully label SPIO with <sup>64</sup>Cu with very high labeling yield. The large surface area of the SPIO enabled labeling with high specific activity which will greatly increase the sensitivity of the detection. The serum stability experiment revealed that the radio-labeled SPIO is stable in mouse serum for up to 24 hours.

## 4.2 Future Work

We recently acquired a new AKTA Purifier equipped with a UV detector and fitted with an in-line radioisotope detector. Future works include verifying the labeling yield and also the RCP (Radio Chemical Purity) with the AKTA Purifier system. It is then necessary to move on to in-vivo mouse model to determine blood circulation half-life and biodistribution of the  $^{64}\text{Cu}$ -labeled SPIO using both small animal PET imaging and a gamma counter to determine activity in organs such as liver, spleen, kidneys and heart. We will further investigate the effect of particle size on biodistribution and blood circulation using PET imaging.

For the cell tracking project, future work includes delivering  $^{64}\text{Cu}$ -labeled SPIO to the hMSCs and tracking the biodistribution of the cells in a mouse model using small animal PET.

## REFERENCES

1. Caravan, P., et al., *Gadolinium(III) Chelates as MRI Contrast Agents: Structure, Dynamics, and Applications*. Chemical Reviews, 1999. **99**(9): p. 2293-2352.
2. Thomsen, H., *Nephrogenic systemic fibrosis: a serious late adverse reaction to gadodiamide*. European Radiology, 2006. **16**(12): p. 2619-2621.
3. Grobner, T., *Gadolinium – a specific trigger for the development of nephrogenic fibrosing dermopathy and nephrogenic systemic fibrosis?* Nephrology Dialysis Transplantation, 2006. **21**(4): p. 1104-1108.
4. Sun, C., J.S.H. Lee, and M. Zhang, *Magnetic nanoparticles in MR imaging and drug delivery*. Advanced Drug Delivery Reviews, 2008. **60**(11): p. 1252-1265.
5. Xie, J., et al., *Ultrasmall c(RGDyK)-Coated Fe<sub>3</sub>O<sub>4</sub> Nanoparticles and Their Specific Targeting to Integrin  $\alpha$ v $\beta$ 3-Rich Tumor Cells*. Journal of the American Chemical Society, 2008. **130**(24): p. 7542-7543.
6. Xu, C. and S. Sun, *Monodisperse magnetic nanoparticles for biomedical applications*. Polymer International, 2007. **56**(7): p. 821-826.
7. Tong, S., et al., *Coating Optimization of Superparamagnetic Iron Oxide Nanoparticles for High T<sub>2</sub> Relaxivity*. Nano Letters, 2010. **10**(11): p. 4607-4613.
8. Gabizon, A., H. Shmeeda, and Y. Barenholz, *Pharmacokinetics of Pegylated Liposomal Doxorubicin: Review of Animal and Human Studies*. Clinical Pharmacokinetics, 2003. **42**(5): p. 419-436.
9. Klibanov, A.L., et al., *Amphipathic polyethyleneglycols effectively prolong the circulation time of liposomes*. FEBS Letters, 1990. **268**(1): p. 235-237.
10. Photos, P.J., et al., *Polymer vesicles in vivo: correlations with PEG molecular weight*. Journal of Controlled Release, 2003. **90**(3): p. 323-334.
11. Andrian, U.H.V. and C. M'rini, *In Situ Analysis of Lymphocyte Migration to Lymph Nodes*. Cell Communication and Adhesion, 1998. **6**(2-3): p. 85-96.
12. Lanzkron, S.M., M.I. Collector, and S.J. Sharkis, *Hematopoietic Stem Cell Tracking In Vivo: A Comparison of Short-Term and Long-Term Repopulating Cells*. Blood, 1999. **93**(6): p. 1916-1921.
13. Hoehn, M., et al., *Monitoring of implanted stem cell migration in vivo: A highly resolved in vivo magnetic resonance imaging investigation of experimental stroke in rat*. Proceedings of the National Academy of Sciences, 2002. **99**(25): p. 16267-16272.
14. Oude Engberink, R.D., et al., *Comparison of SPIO and USPIO for in Vitro Labeling of Human Monocytes: MR Detection and Cell Function I*. Radiology, 2007. **243**(2): p. 467-474.
15. Lewin, M., et al., *Tat peptide-derivatized magnetic nanoparticles allow in vivo tracking and recovery of progenitor cells*. Nature Biotechnology, 2000. **18**(4): p. 410-414.
16. Heymer, A., et al., *Iron oxide labelling of human mesenchymal stem cells in collagen hydrogels for articular cartilage repair*. Biomaterials, 2008. **29**(10): p. 1473-1483.
17. Moore, A., et al., *Tumoral Distribution of Long-circulating Dextran-coated Iron Oxide Nanoparticles in a Rodent Model I*. Radiology, 2000. **214**(2): p. 568-574.
18. Liu, Y. and J. Wang, *Comparative and quantitative investigation of cell labeling of a 12-nm DMSA-coated Fe<sub>3</sub>O<sub>4</sub> magnetic nanoparticle with multiple mammalian cell lines*. Journal of Materials Research, 2011. **26**(06): p. 822-831.
19. Ter-Pogossian, M.M., M.E. Raichle, and B.E. Sobel, *Positron-emission tomography*. Journal Name: Sci. Am.; (United States); Journal Volume: 243:4, 1980: p. Medium: X; Size: Pages: 170-181.
20. Beyer, T., et al., *A Combined PET/CT Scanner for Clinical Oncology*. Journal of Nuclear Medicine, 2000. **41**(8): p. 1369-1379.

21. McCollough, C.H., M.R. Bruesewitz, and J.M. Kofler, *CT Dose Reduction and Dose Management Tools: Overview of Available Options I*. Radiographics, 2006. **26**(2): p. 503-512.
22. Judenhofer, M.S., et al., *PET/MR Images Acquired with a Compact MR-compatible PET Detector in a 7-T Magnet I*. Radiology, 2007. **244**(3): p. 807-814.
23. Seemann, *Whole-body PET/MRI: the future in oncological imaging*. EUROPEAN JOURNAL OF MEDICAL RESEARCH, 2004: p. 309-312.
24. Glaus, C., et al., *In Vivo Evaluation of <sup>64</sup>Cu-Labeled Magnetic Nanoparticles as a Dual-Modality PET/MR Imaging Agent*. Bioconjugate Chemistry, 2010. **21**(4): p. 715-722.
25. Sprague, J.E., et al., *Synthesis, Characterization and In Vivo Studies of Cu(II)-<sup>64</sup>-Labeled Cross-Bridged Tetraazamacrocyclic-amide Complexes as Models of Peptide Conjugate Imaging Agents*. Journal of Medicinal Chemistry, 2007. **50**(10): p. 2527-2535.
26. Jarrett, B.R., et al., *In Vivo Mapping of Vascular Inflammation Using Multimodal Imaging*. PLoS ONE, 2010. **5**(10): p. 1-8.